ELSEVIER

Earth and Planetary Science Letters 164 (1998) 221–232

EPSL

# Late Cretaceous magmatism in Madagascar: palaeomagnetic evidence for a stationary Marion hotspot

T.H. Torsvik [a,b,*], R.D. Tucker [c], L.D. Ashwal [d], E.A. Eide [a], N.A. Rakotosolofo [d], M.J. de Wit [e]

[a] *Geological Survey of Norway, PO Box 3006 Lade, N-7002 Trondheim, Norway*
[b] *Institute of Solid Earth Physics, University of Bergen, N-5002 Bergen, Norway*
[c] *Department of Earth and Planetary Sciences, Washington University, Brookings Drive, St. Louis, MO 63130, USA*
[d] *Department of Geology, Rand Afrikaans University, PO Box 524, Auckland Park, 2006, South Africa*
[e] *Department of Geosciences, University of Cape Town, Rondebosch, 7700, South Africa*

Received 30 June 1998; revised version received 18 September 1998; accepted 21 September 1998

**Abstract**

Late Cretaceous basaltic volcanics in the Morondava Basin (SW Madagascar) possess high-quality and pre-fold palaeomagnetic data (declination 353.5º, inclination −54.8º, $\alpha_{95} = 2.4$º). The palaeomagnetic data are all of normal magnetic polarity, and remanence acquisition is linked to the terminal stages of the Cretaceous Normal Superchron (≥83 Ma). This is sustained by an $^{40}$Ar/$^{39}$Ar age of 83.6 ± 1.6 Ma from one of the tested basaltic flows. A precise U/Pb zircon–baddeleyite age from northeast Madagascar demonstrates magmatism at least back to 91.6 ± 0.3 Ma; thus reliable isotope ages for the Madagascar Cretaceous igneous province span a range of 8 million years. Late Cretaceous palaeomagnetic data obtained from volcanics and dolerites all over Madagascar are directionally concordant, and the combined palaeomagnetic pole (latitude 68.5ºN, longitude 230.3ºE, $A_{95} = 5.5$º, $N = 8$ studies; sampling age range ca. 84–90 Ma) represents one of the best Late Cretaceous poles for the former Gondwanan elements. The collective palaeomagnetic data yield a palaeolatitude of 45.3º$S^{+5.3}_{-4.7}$ for the proposed focal point of the Marion plume (Volcan de l'Androy, southeast Madagascar) during the Late Cretaceous. This is in perfect agreement with hotspot-controlled reconstructions that place the Marion hotspot (46.0ºS) beneath southeast Madagascar during the Late Cretaceous. Setting true polar wander aside, hotspot movements in the Indian Ocean do not appear to exceed ca. 0.75 cm/yr, and the Marion hotspot appears stationary within the resolution power of palaeomagnetic data. 

*Keywords:* Madagascar; Cretaceous; palaeomagnetism; geochronology; hot spots

## 1. Introduction

The assembly of Pangea was completed in Permian–Early Triassic times, but its break-up, commencing with rifting and sea-floor spreading in the Central Atlantic and at the southern margins of Pangea, started in the Mid-Jurassic. Madagascar and India played key roles in this early break-up as they jointly rifted off East Africa at ca. 165 Ma. Sea-floor spreading between Africa and Madagascar probably terminated at ca. 130 Ma [1]. The Cretaceous of Madagascar is characterized by widespread magmatism, related to the Marion hot spot [2,3], which may have been instrumental in the ensuing separation of Madagascar and India.

* Corresponding author. Tel.: +47 73 904011; Fax: +47 73 904494; E-mail: trond.torsvik@ngu.no

0012-821X/98/$ – see front matter 
PII: S0012-821X(98)00206-4

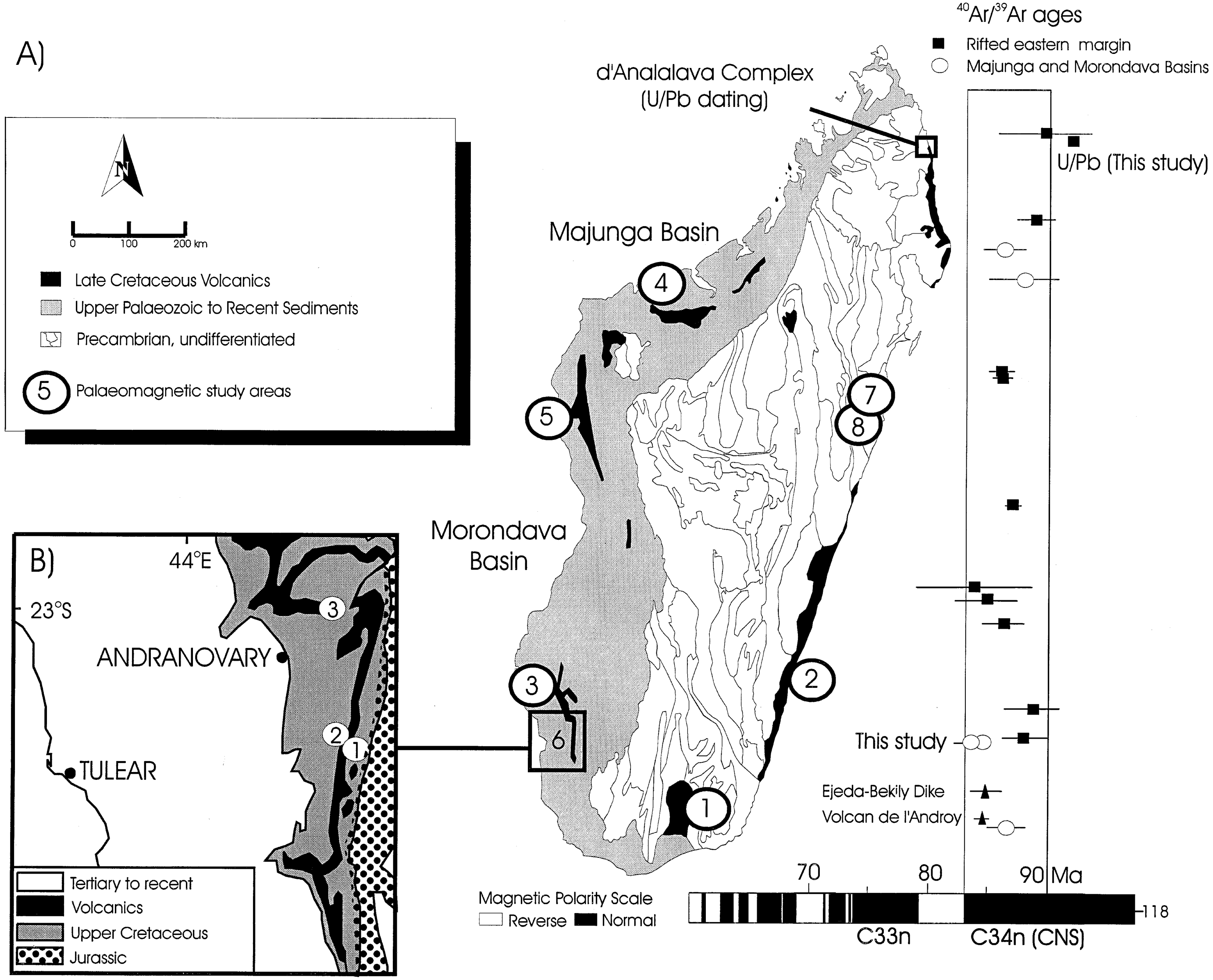


Fig. 1. (A) Simplified geological map of Madagascar highlighting the distribution of Upper Cretaceous volcanics. $^{40}Ar/^{39}Ar$ [3, this study] and U/Pb (d'Analalava gabbro complex; this study) ages (with $2\sigma$ errors) from Cretaceous rocks are shown in approximate latitude position in the right-hand box. Magnetic polarity scale after [7]. Note that all isotopic ages fall within the end of the Cretaceous Normal Polarity Superchron. Large circled numbers show locations of existing palaeomagnetic studies (*1–5* = volcanics, *7–8* = dykes; see Table 4). (B) Geological map of the study area (sites 1–3) for palaeomagnetics and $^{40}Ar/^{39}Ar$ age dating.

As part of a larger project on the assembly and break-up of Pangea, we report new palaeomagnetic and isotopic age data ($^{40}Ar/^{39}Ar$ and U–Pb) for the Cretaceous igneous rocks of Madagascar. Cretaceous palaeomagnetic data exist for Madagascar, but the palaeolatitudinal information from these data was never used to test the Marion hotspot postulate [3]. This may reflect that these palaeomagnetic studies are either unpublished [4], or that the magnetic signatures were considered to represent younger remagnetizations [5]. We will show that the latter remagnetization model is false and, more importantly, that the Cretaceous volcanics from Madagascar in fact can be used to test the Marion hotspot postulate.

## 2. Geological setting

The eastern two thirds of Madagascar consist of variably deformed Precambrian granitoids and subordinate mafic rocks, ranging in age between 3.2 Ga and ca. 550 Ma [6]. The western third of Madagascar comprises extensive, west-dipping Phanerozoic sedimentary rocks within two major basins, referred to as the Majunga and Morondava Basins (Fig. 1). The oldest rocks in the Morondava Basin (Sakoa Group) consist of Late Carboniferous tillites overlain by Early Permian coal-bearing horizons and redbeds, and mid-Permian marine limestones. Unconformably overlying the Sakoa Group is the Sakamena Group, consisting of Late Permian continental sandstones and conglomerates, followed by Early Triassic alternating continental sandstones and marine shales. The Middle Triassic to Early Jurassic Isalo Group unconformably overlies the Sakamena, and consists of sandstones that attain a thickness of over 5 km. Marine conditions began in the Middle Jurassic, represented by interbedded limestones and shales, and mixed marine and continental environments continued into the Early Cretaceous. By the Late Cretaceous (Turonian), marine conditions were dominant, and interbedded basaltic lavas mainly occur between strata of Turonian through Maastrichtian age [8]. Late Cretaceous volcanic and intrusive rocks, including basalt and rhyolite flows, basalt dikes, and small gabbroic plutons, also occur along the eastern rifted margin of Madagascar [3].

## 3. Cretaceous magmatism: isotopic age constraints

Storey et al. [3] proposed short-lived ($\leq$6 Ma) flood basalt and rhyolite volcanism throughout Madagascar, and argued that magmatism first ceased in the north. Their estimate of the time of this Late Cretaceous event is based on seventeen $^{40}Ar/^{39}Ar$ age determinations (both whole-rock step heating and laser fusion measurements of feldspar separates) on flows and dikes from the rifted eastern margin of Madagascar, the Majunga and Morondava Basins, the Volcan de l'Androy massif, and the Ejeda–Bekily dike swarm (Fig. 1). Their preferred ages range between 88.5 $\pm$ 0.6 Ma and 83.7 $\pm$ 5.0 Ma (table 1 of [3]), but special significance was attached to a weighted mean age of 87.6 $\pm$ 0.6 Ma for nine samples from the eastern rifted margin.

In our palaeomagnetic study area (Fig. 1), basaltic lavas overlap continental sandstones and are themselves overlain by limestones, all of Santonian age ([8], 85.8 $\pm$ 0.5 to 83.5 $\pm$ 0.5 Ma following the timescale of [9]). The volcanics in the region of sites 1 and 2 have previously been dated to 84.5 $\pm$ 0.7 Ma [3]. A whole-rock step heating experiment for a site 1 sample (Fig. 2, Table 1) corroborates this age, and we calculate a plateau age of 83.6 $\pm$ 1.6 Ma

Table 1
$^{40}Ar/^{39}Ar$ whole-rock furnace step heating of sample MAD97-1 from site 1 ($j = 0.0061199$, weight 5 mg)

| $T$ (ºC) | $^{39}Ar$ (%) | Age (Ma) |
|---|---|---|
| 600 | 26.9 | 75.4 $\pm$ 0.7 |
| 650 | 40.1 | 83.7 $\pm$ 0.8 |
| 700 | 52.3 | 84.3 $\pm$ 0.8 |
| 750 | 65.4 | 83.9 $\pm$ 0.8 |
| 800 | 76.2 | 83.6 $\pm$ 0.8 |
| 850 | 82.9 | 82.9 $\pm$ 0.8 |
| 900 | 86.3 | 81.2 $\pm$ 0.9 |
| 950 | 88.5 | 78.9 $\pm$ 0.9 |
| 1000 | 90.4 | 76.5 $\pm$ 1.0 |
| 1050 | 93.0 | 82.4 $\pm$ 0.9 |
| 1100 | 97.4 | 91.2 $\pm$ 0.9 |
| 1150 | 99.6 | 87.2 $\pm$ 1.0 |
| 1200 | 100 | 87.1 $\pm$ 3.8 |

Individual temperature steps are listed with 1$\sigma$ errors (excluding $J$). A weighted mean plateau age of 83.6 $\pm$ 1.6 Ma (2$\sigma$ error including $J$) was calculated for temperature steps 650–850 (56% gas). Analytical protocol follows [10].

Table 2
U–Pb dilution analyses, d'Analalava Complex

| Fractions | | Concentrations | | | | | Atomic ratios | | | | Age (Ma) |
|---|---|---|---|---|---|---|---|---|---|---|---|
| No. | Properties [a] | Wt. [b] ($\mu$g) | Pb rad [b] (ppm) | U [b] (ppm) | Pb com [c] (pg) | Th/U [d] | $^{206}Pb/^{204}Pb$ [e] | $^{207}Pb/^{207}Pb$ [f] | $^{207}Pb/^{235}U$ [f] | $^{206}Pb/^{238}U$ [f] | $^{206}Pb/^{238}U$ [f] |
| *Coarse gabbro-norite* | | | | | | | | | | | |
| 1 | Zr,3,+200,cl,c,sk | 7 | 7.35 | 230 | 2.5 | 4.62 | 597.7 | 0.04802 ± 44 | 0.0953 ± 9 | 0.01439 ± 5 | 92.1 ± 0.3 |
| 2 | Zr,3,+200,cl,c,sk | 10 | 4.03 | 143 | 2.3 | 4.13 | 608.6 | 0.04767 ± 20 | 0.0943 ± 4 | 0.01436 ± 3 | 91.9 ± 0.2 |
| 3 | Zr,5,+200,cl,c,sk | 13 | 8.15 | 298 | 2.4 | 3.66 | 1435 | 0.04779 ± 9 | 0.0945 ± 2 | 0.01434 ± 2 | 91.8 ± 0.1 |
| 4 | Zr,7,+200,cl,c,sk | 20 | 5.69 | 178 | 3.6 | 5.06 | 953.7 | 0.04771 ± 25 | 0.0944 ± 5 | 0.01435 ± 3 | 91.9 ± 0.2 |
| 5 | B,14,−200,pb,cl,pl | 84 | 2.22 | 168 | 5.1 | 0.079 | 3273 | 0.04788 ± 5 | 0.0941 ± 1 | 0.01425 ± 2 | 91.2 ± 0.1 |
| 6 | B,10,+200,pb,cl,pl | 27 | 1.95 | 149 | 3.0 | 0.033 | 1245 | 0.04778 ± 11 | 0.0939 ± 2 | 0.01425 ± 3 | 91.2 ± 0.2 |
| 7 | B,20,−200,pb,cl,pl | 59 | 1.90 | 142 | 5.3 | 0.123 | 1456 | 0.04781 ± 12 | 0.0941 ± 2 | 0.01428 ± 3 | 91.4 ± 0.2 |
| 8 | B,31,−200,pb,cl,pl | 84 | 2.22 | 169 | 5.1 | 0.079 | 2575 | 0.04788 ± 5 | 0.0941 ± 1 | 0.01425 ± 2 | 91.2 ± 0.1 |

[a] Zr = zircon, B = baddeleyite. Cardinal number indicates the number of zircon grains anlyzed (e.g. 25 grains); all grains were selected from non-paramagnetic separates at 0º tilt at full magnetic field in a Frantz Magnetic Separator; +200 = size in mesh (>75 $\mu$m); c = colorless; cl = clear; pl = platey; pb = pale brown; sk = skeletal. All zircon analyses were abraded after [11]; baddeleyite was not abraded.
[b] Concentrations are known to ±30% for sample weights of about 20 $\mu$g and ±50% for samples ≤5 $\mu$g.
[c] Corrected for 0.0215 mole fraction common-Pb in the $^{205}Pb$–$^{235}U$ spike.
[d] Calculated Th/U ratio assuming that all $^{208}Pb$ in excess of blank, common-Pb, and spike is radiogenic ($\lambda^{232}Th = 4.9475 \times 10^{-11}$ $y^{-1}$).
[e] Measured, uncorrected ratio.
[f] Ratio corrected for fractionation, spike, blank, and initial common-Pb (at the determined age from [12]). Pb fractionation correction = 0.094%/amu (±0.025%, $1\sigma$); U fractionation correction = 0.111%/amu (±0.02%, $1\sigma$); U blank = 0.2 pg; Pb blank ≤10 pg. Absolute uncertainties $(1\sigma)$ in the Pb/U and $^{207}Pb/^{206}Pb$ ratios calculated following [13]. This column lists the $^{206}Pb/^{238}U$ age ($\pm 1\sigma$ absolute), which is considered more accurate. U and Pb half-lives and isotopic abundance ratios from [14].

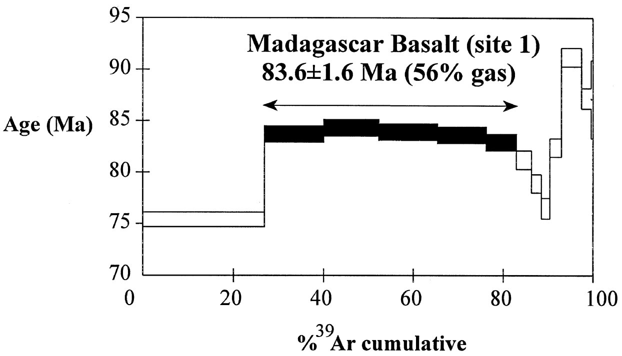


Fig. 2. $^{40}$Ar–$^{39}$Ar whole-rock spectrum for a basaltic sample (site 1, see Fig. 1) that shows apparent age as a function of the cumulative fraction of $^{39}$Ar released (Table 1). Height of boxes indicates analytical error ($\pm 1\sigma$) about each step. The $^{40}$Ar/$^{39}$Ar laboratory at Stanford University was used; samples were irradiated at the Oregon State University reactor. Analytical protocol follows [10]. We cite uncertainties at the $2\sigma$ level and include uncertainties in $J$-value for the $83.6 \pm 1.6$ Ma plateau age (filled boxes). Individual steps were weighted by both length (gas volume) and individual age uncertainty.

($2\sigma$ error including $J$) which is concordant with the previous age of [3]. Both ages agree well with the stratigraphic (Santonian) age estimate.

We also dated zircon and baddeleyite from the d'Analalava gabbro (65 km$^2$) in northeast Madagascar (Fig. 1). This body is one of several igneous complexes of presumed Late Cretaceous age that underlies, and is a probably magma chamber to, the basalt and rhyolite volcanics along the eastern margin of Madagascar. Our sample is a medium- to coarse-grained olivine gabbronorite collected from a road gravel quarry approximately 20 km south of Vohemar. All analyses are concordant at a common age within cited errors (Fig. 3, Table 2), but because of the young age and the fact that $^{206}$Pb/$^{238}$U is less susceptible to correction procedures, we cite a weighted mean $^{206}$Pb/$^{238}$U age of $91.6 \pm 0.3$ Ma for all analyses as the most reliable age estimate. This age is within error of the 89.3±3.9 Ma $^{40}$Ar/$^{39}$Ar age of basaltic volcanics from the same region (Fig. 1). If related, the U/Pb age most closely represents the true emplacement age.

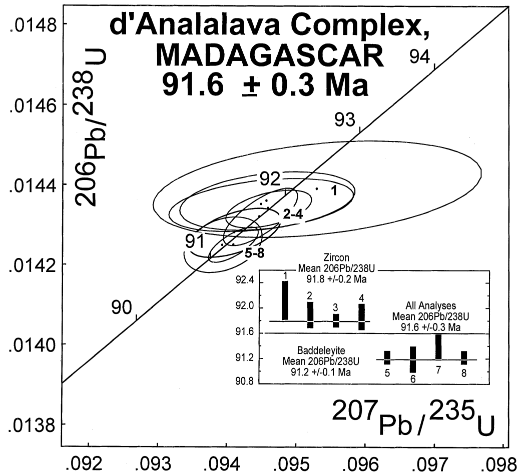


Fig. 3. Concordia diagram showing isotope dilution analyses of zircon (analyses *1–4*) and baddeleyite (analyses *5–8*) of the d'Analalava gabbro (see location in Fig. 1). All analyses are concordant within analytical error (shown as $2\sigma$ in the figure). The zircons, however, have a slightly older age with a weighted mean $^{206}$Pb/$^{238}$U age of $91.8 \pm 0.2$ Ma; the four baddeleyite analyses have a mean $^{206}$Pb/$^{238}$U age of $91.2 \pm 0.1$ Ma.

## 4. Palaeomagnetic experiments

Basaltic lava flows from three palaeomagnetically tested sites in the Morondava Basin (Fig. 1) are dominantly fresh, with only minor alteration. Samples from sites 1 and 2 contain randomly oriented plagioclase laths and needles, which commonly show minor compositional zoning. Interstitial augite is pale-green, probably indicative of low-$TiO_2$ content. Fe–Ti oxides occur as subhedral to euhedral grains and randomly oriented needles. The groundmass is extremely fine-grained and contains minor glass. Minor Fe-hydroxides occur as vesicle fillings and minor patches disseminated throughout the rocks. Site 3 samples contain randomly oriented plagioclase microlites, small augite crystals and disseminated Fe–Ti oxides in a dark, glassy matrix, all of which indicate relatively rapid cooling. Minor Fe-hydroxide alteration is also present in this sample.

Opaque minerals in basalt samples from sites 1 and 2 consist of homogeneous ilmenite and titanomagnetite (TM), both as discrete euhedral to subhedral grains or as composite grains. In addition, randomly oriented needles of TM up to 100 μm long, and with length : width ratios varying between 25 : 1 and 30 : 1 occur throughout the rocks. A small population of TM grains have been partly or completely altered to titanomaghemite, representing low-temperature oxidation. There is no evidence for high-temperature oxidation effects. Site 3 samples contain ilmenite needles and skeletal, cruciform TM crystals, which commonly occur as elongated chains of multiple crystals. Some TM contain thin cracks along which titanomaghemite has developed during low-temperature oxidation.

The natural remanent magnetization (NRM) was measured on a JR5A magnetometer, and stability of NRM was tested by thermal (furnace model MMT-D60) and alternating field (AF) demagnetization. Characteristic remanence components were calculated with the least square regression analysis implemented in the SIAPD computer program (available at http://www.ngu.no/geophysics).

Demagnetization experiments disclose high-unblocking components with steep negative inclination and ENE (site 1) or northerly declination (sites 2 and 3; Fig. 4, in-situ coordinates). Discrete unblocking in the 250–350ºC range is frequently observed, and at site 3, remanence stability vanished at 350–400ºC (Fig. 4A). Conversely, samples from sites 1 and 2 possessed remanence stability up to 530–560ºC. Low-unblocking components are typically demagnetized at low temperatures or low AF fields (Fig. 4B).

Thermomagnetic analyses (TMA) yield metastable phases with low Curie temperatures ($T_c \approx 300$ºC), followed by unmixing (inversion) and a second $T_c$ at ca. 550ºC (Fig. 4C–D). TMA curves are typical of oceanic basalts and suggest TM and/or low-temperature oxidized TM (titanomaghemites), consistent with petrographic observations that show predominantly homogeneous TM with only minor low-temperature alteration (titanomaghemite). High resistance to AF demagnetization (>95 mT, Fig. 4B) could relate to the TM needles described above.

## 5. Interpretation of palaeomagnetic data

NRM scatter for the basaltic volcanics is quite reduced after demagnetization, and bedding correction improves remanence grouping considerably (Fig. 4E–G, Table 3). The fold-test (strictly a tilt-test) is statistically significant at the 95% confidence level, and the bedding-corrected directions compare well with the existing Late Cretaceous palaeomagnetic results from Madagascar (Fig. 4H, Table 4). On a local level, our data compare with those of [4] (his table V-5, p. 141; sites Vineta, Anketa and Vatolatsaka), although it is unclear if corrections, however minor, were made for local bedding orientation.

All Late Cretaceous igneous rocks from Madagascar yield normal polarity magnetizations; this should be expected if magnetizations are primary since reliable isotopic ages from palaeomagnetically tested

Table 3
Palaeomagnetic results from Late Cretaceous volcanics (Santonian, 84.5 ± 0.7 Ma [3] and 83.6 ± 1.6 Ma, site 1 of this study)

| $N$ (sites) | P | In-situ | | | | Unfolded | | | |
|---|---|---|---|---|---|---|---|---|---|
| | | Dec. (º) | Inc. (º) | $\alpha_{95}$ | $k$ | Dec. (º) | Inc. (º) | $\alpha_{95}$ | $k$ |
| 41 (3) | N | 340.3 | −62.1 | 4.3 | 28.4 | 353.5 | −54.8 | 2.4 | 91.1[a] |
| | | | | | (pole = 76.8ºN, 248.2ºE; $dp/dm = 2.4º/3.4º$) | | | | |

$N$ = number of samples (sites); P = polarity (N = normal, R = reverse); Dec./Inc. = mean declination/inclination; $\alpha_{95}$ = 95% confidence circle; $k$ = precision parameter; pole = palaeomagnetic pole (unfolded co-ordinates); $dp/dm$ = semi-axes of the cone of 95% confidence about the pole.

[a] Positive fold-test at 95% confidence level.

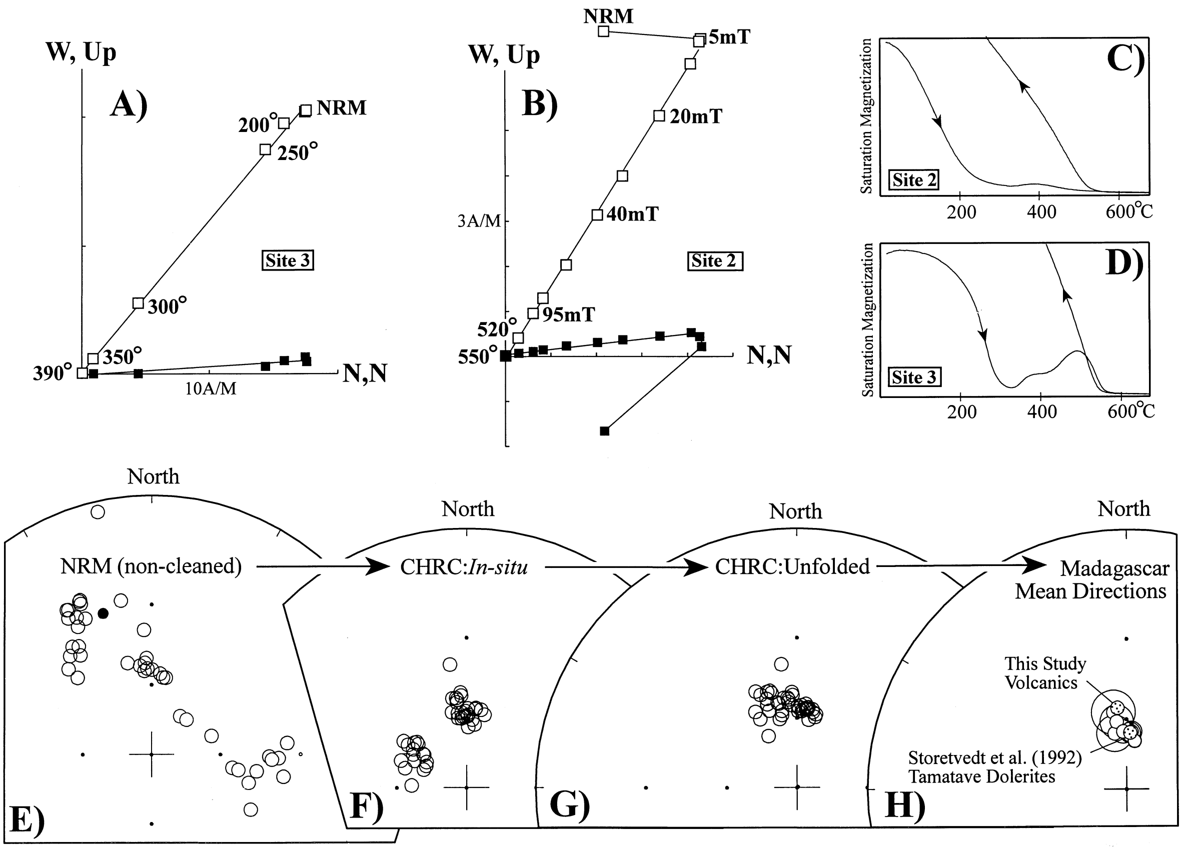


Fig. 4. (A)Thermal demagnetization of a site 3 sample (in-situ co-ordinates). (B) AF demagnetization of a site 2 sample followed by thermal demagnetization; remanence stability exceeded the maximum available AF field (95 mT) (in-situ co-ordinates). (C) Thermomagnetic analysis (in air) for a site 2 sample (magnetic field = 500 mT). (D) Thermomagnetic analysis for a site 3 sample. Note stronger unmixing/inversion during heating and higher saturation magnetization during cooling. (E–G) Stereoplots of individual sample directions (this study) showing progressively better grouping from NRM uncleaned sample-directions (E), CHRC's (cleaned) in-situ (F) and finally well-grouped tectonically corrected (unfolded) CHRC's (G). (H) Comparison of mean directions and associated $\alpha_{95}$ confidence circles from this study and existing results (Table 4). Existing mean directions have been recalculated to a common geographic site (latitude 23.3ºS, longitude 44.4ºE). In vector diagrams, open (closed) symbols represent points in the vertical (horizontal) plane. In stereoplots, open (closed) symbols denote upward (downward) pointing inclinations. *ChRC* = characteristic remanence component.

rocks all fall within the Cretaceous Normal Superchron (CNS, 83–118 Ma; [7]). From the anticipated normal polarity and a positive fold-test (this study), we argue for a near-primary origin of magnetization for the Late Cretaceous rocks of Madagascar. Given the small isotopic age differences, it is not surprising that all Late Cretaceous palaeomagnetic data are concordant at the 95% confidence level (insignificant apparent polar wander). We therefore combined all results to calculate a mean Late Cretaceous palaeomagnetic pole for Madagascar (Fig. 5, Table 4).

Our interpretation of the Late Cretaceous data as primary magnetizations contrasts to that of Storetvedt et al. [5], who suggested that a long-lasting (ca. 40 Ma) Madagascar-wide overprint event occurred during Late Cretaceous and Tertiary times. We find this unlikely since (1) this proposed and continuous remagnetization 'event' spans about 15 magnetic field reversals, whilst all the Late Cretaceous rocks show normal polarity, and (2) Neoproterozoic granites and Palaeozoic–Mesozoic sedimentary sequences all over Madagascar yield dual-polarity directions (e.g. [17,18]), at variance with the Late

Table 4
Summary of Late Cretaceous (ca. 84−90 Ma) palaeomagnetic data from Madagascar ($Q \geq 3$)

| Rock unit and location | Dec. (º) | Inc. (º) | $\alpha_{95}$ | Glat | Glong | Plat | Plong | $dp/dm$ | $Q$ | Ref. |
|---|---|---|---|---|---|---|---|---|---|---|
| *Volcanics* | | | | | | | | | | |
| 1. Massif d'Androy | 348.8 | −66.2 | 7.6 | −24.2 | 46.0 | 64.0 | 243.0 | 10.2/12.5 | 4 | [4] |
| 2. Southeast coast | 007.1 | −63.6 | 4.4 | −21.8 | 48.0 | 65.8 | 215.6 | 5.5/7.0 | 4 | [4] |
| 3. Mangoky-Anilahy | 350.3 | −56.1 | 8.9 | −22.8 | 44.3 | 73.7 | 253.1 | 9.2/12.8 | 4 | [4] |
| 4. Antanimena | 358.0 | −59.4 | 4.9 | −16.4 | 46.0 | 66.1 | 229.7 | 5.5/7.4 | 4 | [4] |
| 5. Mailaka | 352.2 | −55.8 | 6.9 | −18.0 | 44.4 | 70.3 | 243.1 | 7.1/9.9 | 4 | [4] |
| 6. SW Madagascar | 353.5 | −54.8 | 2.4 | −23.2 | 44.3 | 76.8 | 248.2 | 2.4/3.4 | 6 | this study |
| *Dolerites* | | | | | | | | | | |
| 7. Tamatave | 10.6 | −64.5 | 2.8 | −18.0 | 47.0 | 60.2 | 212.1 | 3.6/4.5 | 3 | [4] |
| 8. Tamatave | 006.0 | −61.0 | 4.3 | −18.0 | 47.0 | 65.5 | 218.0 | 5.5/6.8 | 5 | [5] |
| Mean Late Cretaceous volcanics and dolerites | | | | | | 68.5 | 230.3 | $A_{95} = 5.5$ | $N = 8$ | |

Glat/Glong = geographic latitude/longitude; Plat/Plong = palaeomagnetic pole latitude (north)/longitude (east); $Q$ = quality factor [15]; Ref = reference, $A_{95}$ = 95% confidence circle around the mean pole. See Fig. 1 for locations and Table 3 for further legend.

Cretaceous directions. This argues strongly against extensive continental-scale remagnetization of the Madagascar sequences.

## 6. Hotspot migration

Palaeomagnetic data from Madagascar testify to a Late Cretaceous palaeolatitude of ca. 47ºS for the southern tip of Madagascar (Fig. 5). This latitude estimate is consistent with hotspot reconstructions [16] that place southeast Madagascar above the Marion hotspot (46.0ºS, 37.8ºE) at 90 Ma, and at about 120 km north of Marion at 84 Ma (chron 34; Fig. 5). Subsequently, India and the Seychelles (part of Greater India) drifted NNE away from Madagascar, and finally separated from one another over the Reunion hotspot (Fig. 6A) that produced the massive Deccan traps at the K–T boundary.

Hotspots offer a unique contribution to palaeoreconstructions since they provide palaeolongitudinal control on plate positions (absolute reference scheme), in contrast to reconstructions based on palaeomagnetic data alone (unknown palaeolongitude). A fundamental assumption, however, is that hotspots are stationary or move at insignificant speeds relative to plate-tectonic speeds. Discrepancies between hotspot and palaeomagnetic reference frames have traditionally been explained by true polar wander (TPW) driven by changes in the Earth's moment of inertia, or simply the fact that hotspots may not be as stationary as often granted [24,25]. For example Tarduno and Cottrell [24] argue that the Hawaii hotspot has moved southward at speeds approximating 3 cm/yr, while the global mantle circulation model of Steinberger and O'Connell [25] predicts migration rates at 1.2 cm/yr. In light of our results that suggest that the Marion hotspot is 'stationary' within the resolution power of palaeomagnetically derived latitudes, we will briefly analyse the palaeomagnetic evidence for hotspot migration in the Indian Ocean.

It is well known that the present latitude of the Reunion hotspot (21.1ºS and 55.5ºE, Fig. 6A) does not fully correspond with palaeomagnetic latitudes derived from the Deccan Traps in India. Taken at face value, and ignoring TPW, the Deccan palaeomagnetic data [19] require a northward component of 450–500 km (Fig. 6B) and a mean northward velocity of 0.7–0.8 cm/yr for the Reunion hotspot, compared to the hotspot reference frame of [16]. This velocity estimate for the hotspot is 3–4 times higher than that predicted by [25] (0.2 cm/yr).

Another target for palaeomagnetic testing of hotspot mobility is the Early Cretaceous (ca. 117 Ma) Rajmahal basalts in eastern India. In this case, coherent palaeomagnetic data yield Early Cretaceous palaeolatitudes of 45.4º$S^{+5.8}_{-4.3}$. This palaeolatitude estimate (Fig. 6C) is within the range of the latitude of the Kerguelen hotspot (ca. 49ºS and 69.5ºE), orig-


Fig. 5. Late Cretaceous hotspot controlled reconstruction at ca. 84 Ma (reconstruction parameters of [16]). Late Cretaceous palaeomagnetic reconstruction of Madagascar (in white) according to a mean north pole of 68.5ºN and 230.3ºE (Table 4; age range of palaeomagnetically studied rocks ca. 84–90 Ma). Note the latitudinal match of the hotspot and the palaeomagnetically controlled reconstruction (longitude unconstrained in the palaeomagnetic frame and Madagascar plotted in an arbitrarily longitude position). The mean Late Cretaceous palaeomagnetic pole from Madagascar is plotted as a south pole (listed as north pole in Table 4) with $A_{95}$ confidence circle. Locations of the Tristan (South Atlantic), Marion and Reunion hotspots (Indian Ocean) are shown.

inally linked to the Rajmahal basalts ([26] and references therein). However, Curray and Munasinghe [27] have suggested that the Rajmahal province was instead attributed to activity of the Crozet plume (ca. 46.3ºS, 51ºE, Fig. 6A). If the Rajmahal basalts are plume-related, then given the unknown palaeolongitude of palaeomagnetic data, both the Kerguelen and the Crozet plume (best fit) present viable linkages (Fig. 6c). [16] place the Kerguelen hotspot ca. 1000 km south of the Rajmahal igneous province in the Early Cretaceous (Fig. 6C); accepting this reconstruction, with the Rajmahal province thus located near the plume-edge boundary, requires a ca. 890 km northward shift of Kerguelen, compared to the palaeomagnetic reference scheme since the Early Cretaceous (Fig. 6C). Incidentally, this mean northward velocity estimate of ca. 0.75 cm/yr for Kerguelen compares with the Reunion migration estimate, but a northerly sense of movement for the Kerguelen hotspot would be opposite of that predicted by [25].

Given the apparent disagreement over which plume, if any, is responsible for the Early Cretaceous Rajmahal igneous activity [26], migration estimates for the Kerguelen hotspot (alternatively Crozet [27]) should be treated cautiously. Setting Kerguelen aside, current evidence from the Indian Ocean therefore favours an almost stationary Marion hotspot while the Reunion hotspot might have migrated 450–500 km northward since the Early Tertiary.

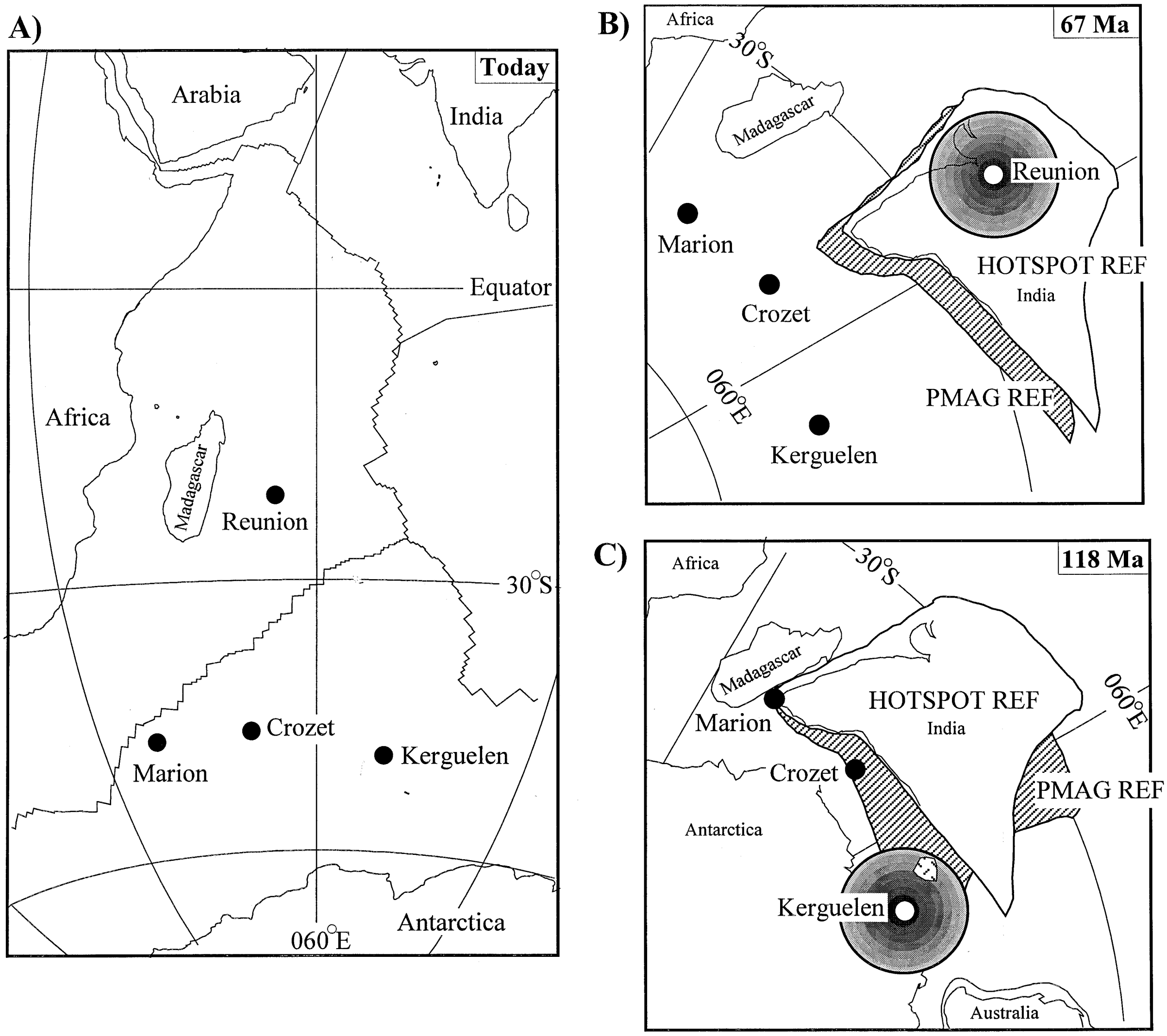


Fig. 6. (A) Map of Africa, Arabia, India, Madagascar and Antarctica, present plate boundaries, and the location of the Marion, Crozet, Kerguelen and Reunion hotspots. (B) Comparison of a hotspot [16] and palaeomagnetically (*PMAG REF*) controlled reconstruction of India at the K–T boundary. Position of India (arbitrary longitude) according to a mean palaeomagnetic pole from the Deccan Traps (pole latitude 36.9°N, longitude 281.3°E, $A_{95} = 2.4°$ [19]). The location of Marion, Crozet and the Kerguelen hotspots are shown. (C) Comparison of a hotspot [16] and palaeomagnetically (*PMAG REF*) controlled reconstruction of India during the Early Cretaceous. Position of India according to a mean palaeomagnetic pole of 8°N, 297.8°E and $A_{95} = 4.7°$ (calculated from [15,20–23]) from the Rajmahal basalts, eastern India (palaeomagnetic study area indicated in PMAG REF figure as small grey shaded polygon). Once again longitude is arbitrary in the palaeomagnetic reconstruction.

## 7. Conclusions

Late Cretaceous volcanism in Madagascar has been attributed to magmatic activity above the Marion hotspot [2,3,28], and $^{40}Ar/^{39}Ar$ ages range between ca. 84 and 90 Ma for the postulated Marion hotspot-related magmatism. A precise U/Pb zircon–baddeleyite age, however, from northeast Madagascar demonstrates magmatic activity at least back to 91.6 ± 0.3 Ma, and reliable isotope ages thus span a range of 8 Ma (83.6–91.6 Ma).

Late Cretaceous volcanics and dolerites from

Madagascar yield directionally concordant magnetizations, all of normal polarity, and are argued above to record near-primary magnetic signatures within the upper part of the CNS. The collective palaeomagnetic data yield one of the best Late Cretaceous poles from the former Gondwanan elements, and testify to a palaeolatitude of 47ºS for the southern tip of Madagascar (Fig. 5). This latitude estimate is in excellent agreement with hotspot reconstructions [16]. Storey et al. [3] suggested that the Volcan de l'Androy in southeast Madagascar (Fig. 1) marked the focal point of the Marion plume at ca. 88 Ma. With reference to the Volcan de l'Androy (located at 24.2ºS and 46ºE), the palaeomagnetic data yield a palaeolatitude of $45.3^{\circ}S^{+5.3}_{-4.7}$ and are in excellent agreement with the present latitude of the Marion hotspot (46.0ºS).

## Acknowledgements

The Norwegian Research Council, the Geological Survey of Norway, the National Science Foundation (USA) and the Foundation for Research Development (RSA) is thanked for financial support. ***[RV]***

## References

[1] M.F. Coffin, P.D. Rabinowitz, Evolution of the conjugate East African–Madagascan margins and the western Somali Basin, Geol. Soc. Am. Spec. Pap. 226 (1988) 78 pp.
[2] J. Mahoney, C. Nicollet, C. Dupuy, Madagascar basalts: tracking oceanic and continental sources, Earth Planet. Sci. Lett. 104 (1991) 350–363.
[3] M. Storey, J.J. Mahoney, A.D. Saunders, R.A. Duncan, S.P. Kelley, M.F. Coffin, Timing of hot spot-related volcanism and the break-up of Madagascar and India, Science 267 (1995) 852–855.
[4] C.R.A. Andriamirado, Recherches paléomagnétiques sur Madagascar: résultats et interprétations dans le cadre de la dislocation de la partie orientale du Gondwana, Ph.D. Thesis, University of Strasbourg, 1971, 202 pp. with annexes.
[5] K.M. Storetvedt, J.G. Mitchell, M.C. Abranches, D. Maaloe, G. Robin, The coast-parallel dolerite dykes of east Madagascar; age of intrusion, remagnetization and tectonic aspects, J. Afr. Earth Sci. 15 (1992) 237–249.
[6] R.D. Tucker, M.J. Handke, M.A. Hamilton, L.D. Ashwal, M. Le Grange, R.A. Rambeloson, U–Pb geochronology and isotope geochemistry of the Archean and Proterozoic Igneous rocks of Madagascar, J. Geol. (1998) (in press).
[7] S.C. Cande, D.V. Kent, Revised calibration of the geomagnetic polarity timescale for the Late Cretaceous and Cenozoic, J. Geophys. Res. 100 (1995) 6093–6095.
[8] H. Besairie, M. Collignon, Géologie de Madagascar, I: Les terrains sédimentaires, Ann. Geol. Madagascar 35 (1972) 553 pp.
[9] F.M. Gradstein, F.P. Agterberg, J.G. Ogg, J. Hardenbol, P. Van Veen, J. Thierry, Z. Huang, A Triassic, Jurassic and Cretaceous time scale, in: W.A. Berggren, D.V. Kent, M.P. Aubry, J. Hardenbol (Eds.), Geochronology, Time Scales and Global Stratigraphic Correlation, SEPM, Spec. Publ. 54 (1995) 95–126.
[10] B.R. Hacker, Q. Wang, Ar/Ar geochronology of ultrahigh-pressure metamorphic rocks in central China, Tectonics 14 (1995) 994–1006.
[11] T.E. Krogh, Improved accuracy of U–Pb zircon ages by the creation of more concordant systems using an air-abrasion technique, Geochim. Cosmochim. Acta 46 (1982) 637–649.
[12] J.S. Stacey, J.D. Kramers, Approximation of terrestrial lead isotope evolution by a two-stage model, Earth Planet. Sci. Lett. 26 (1975) 207–221.
[13] K.R. Ludwig, Calculation of uncertainties of U–Pb istope data, Earth Planet. Sci. Lett. 46 (1980) 212–220.
[14] A.H. Jaffey, K.F. Flynn, L.E. Glendenin, W.C. Bentley, A.M. Essling, Precision measurement of half-lives and specific activities of $^{235}U$ and $^{238}U$, Phys. Rev. Sect. C, Nucl. Phys. 4 (1971) 1889–1906.
[15] C. Radhakrishnamurthy, Remanent Magnetism of Igneous Rocks in the Gondwana Formations of India, Dr. Sci. Thesis, Andra University, 1963, 149 pp.
[16] R.D. Müller, J.-Y. Royer, L.A. Lawver, Revised plate motions relative to the hotspots from combined Atlantic and Indian Ocean hotspot tracks, Geology 21 (1993) 275–278.
[17] M.W. McElhinny, B.J.J. Embleton, L. Daly, J.-P. Pozzi, Paleomagnetic evidence for the location of Madagascar in Gondwanaland, Geology 4 (1976) 455–457.
[18] J.G. Meert, T.H. Torsvik, E.A. Eide, A. Nedelec, A palaeomagnetic review of Gondwana assembly including preliminary palaeomagnetic results from Madagascar (abstract), Gondwana Res. Group Misc. Publ. 5 (1997) 52.
[19] D. Vandamme, V. Courtillot, J. Besse, Paleomagnetism and age determinations of the Deccan Traps (India). Results of a Nagpur–Bombay traverse and review of earlier work, Rev. Geophys. 29 (1991) 159–190.
[20] I. McDougall, M.W. McElhinny, The Rajmahal Traps of India — K–Ar ages and palaeomagnetism, Earth Planet. Sci. Lett. 9 (1970) 371–378.
[21] C.T. Klootwijk, Palaeomagnetism of the Upper Gondwana Traps, northeast India, Tectonophysics 12 (1971) 449–467.
[22] A.K. Das, J.D.A. Piper, G. Banyopadhyay, S.B. Mallik, Polarity inversion in the Rajmahal lavas, north-east India: trap emplacement near commencement of the Cretaceous Normal Superchron, Geophys. J. Int. 124 (1996) 427–452.
[23] G.V.S. Poornachundra Rao, J. Mallikarjuna Rao, Palaeomagnetism of the Rajmahal Traps of India: implications to the Cretaceous Normal Superchron, J. Geomagn. Geoelectr. 48 (1996) 993–1000.

[24] J.A. Tarduno, R.D. Cottrell, Paleomagnetic evidence for motion of the Hawaiian hotspot during formation of the Emperor seamounts, Earth Planet. Sci. Lett. 153 (1997) 171–180.
[25] B. Steinberger, R.J. O'Connell, Advection of plumes in mantle flow: implications for hotspot motion, mantle viscosity and plume distribution, Geophys. J. Int. 132 (1998) 412–434.
[26] W. Kent, A.D. Saunders, P.D. Kempton, N.C. Ghose, Rajmahal Basalts, Eastern India: mantle sources and melt distribution at a volcanic rifted margin, in: J.J. Mahoney, M.F. Coffin (Eds.), Large Igneous Provinces: Continental, Oceanic, and Planetary Flood Volcanism, Am. Geophys. Union, Geophys. Monogr. 100 (1997) 145–182.
[27] J.R. Curray, T. Munasinghe, Origin of the Rajmahal Traps and the 85ºE Ridge: preliminary reconstructions of the trace of the Crozet hotspot, Geology 19 (1991) 1237–1240.
[28] M. Storey, J.J. Mahoney, A.D. Saunders, Cretaceous basalts in Madagascar and the transition between plume and continental lithosphere mantle sources, in: J.J. Mahoney and M.F. Coffin (Eds.), Large Igneous provinces: Continental, Oceanic, and Planetary Flood Volcanism, Am. Geophys. Union, Geophys. Monogr. 100 (1997) 95–122.